Wind and Structures, Vol. 16, No. 2 (2013) 157-178
DOI: http://dx.doi.org/10.12989/was.2013.16.2.157

Output-only modal parameter identification for force-embedded acceleration data in the presence of harmonic and white noise excitations

C.J. Ku*[1], Y. Tamura[1], A. Yoshida[1], K. Miyake[2] and L.S. Chou[3]

[1]*Department of Architectural Engineering, Tokyo Polytechnic University, Iiyama, Japan*
[2]*MHS Planners, Architects & Engineers, Tokyo, Japan*
[3]*Yuh-Ing Junior College of Health Care & Management, General Education Center, Kaohsiung, Taiwan*

(Received November 4, 2010, Revised December 2, 2011, Accepted December 6, 2011)

Abstract. Output-only modal parameter identification is based on the assumption that external forces on a linear structure are white noise. However, harmonic excitations are also often present in real structural vibrations. In particular, it has been realized that the use of forced acceleration responses without knowledge of external forces can pose a problem in the modal parameter identification, because an external force is imparted to its impulse acceleration response function. This paper provides a three-stage identification procedure as a solution to the problem of harmonic and white noise excitations in the acceleration responses of a linear dynamic system. This procedure combines the uses of the mode indicator function, the complex mode indication function, the enhanced frequency response function, an iterative rational fraction polynomial method and mode shape inspection for the correlation-related functions of the force-embedded acceleration responses. The procedure is verified via numerical simulation of a five-floor shear building and a two-dimensional frame and also applied to ambient vibration data of a large-span roof structure. Results show that the modal parameters of these dynamic systems can be satisfactorily identified under the requirement of wide separation between vibration modes and harmonic excitations.

Keywords: acceleration; ambient vibration; correlation; excitations; frequency response; identification; modal model; mode indication function

1. Introduction

A modal model with a limited number of parameters has been proven to be very beneficial in evaluating structural performance for a linear dynamic system. To establish the modal model, acceleration response measurement provides an efficient and essential tool in engineering fields, because of its convenience of use. The information in the modal model, consisting of natural frequency, damping ratio, and mode shape, are extracted from the measured acceleration response data by means of output-only modal parameter identification. Approaches to modal parameter identification are generally categorized into frequency domain techniques and time domain techniques. Most frequency domain identification techniques are based on the fast Fourier

*Corresponding author, Former Global COE Researcher, E-mail: ku@arch.t-kougei.ac.jp

transform (FFT) algorithm developed in the late 1960s. FFT enables rapid calculation of frequency response functions (FRFs) from external forces and resultant responses for a linear dynamic system. In developing frequency domain techniques, time domain techniques have been used as alternative approaches. One common approach is the random decrement (RD) technique (Cole 1971).

The RD technique was developed to form a characteristic signature, an RD signature of a dynamic system, based on the ensemble average of pre-selected sample segments from output-only random responses. The RD signature can be used to continue with modal parameter identification when it resembles a free vibration response of a linear dynamic system. Under the assumption of Gaussian white noise excitations and certain initial conditions of the dynamic system, the equivalent relation between the RD signatures and the free vibration responses has been derived theoretically from displacement and velocity responses (Vandiver *et al*. 1982, Bedewi 1986). However, non-equivalence between acceleration-based RD signatures and free vibration responses, because a singular point exists in the RD signatures, has been shown (Huang and Yeh 1999).

A singular point arises from the RD signature of the white noise excitation to the dynamic system. Likewise, when a color noise excitation is applied to a dynamic system, the acceleration-based RD signature deviates from its free vibration response due to the RD signatures of the applied force (Ku 2004). In fact, the same issue can be raised for the use of the correlation function, because the RD signature is known to be proportional to its correlation function. Using the correlation-related functions of the acceleration responses in a time domain identification technique can thus pose the problem of identification accuracy of the modal parameters, especially for the damping estimates (Ku *et al*. 2007a, Ku *et al*. 2007b, Ku and Tamura 2009).

A straightforward strategy for tackling the singular problem in the correlation-related functions would be simultaneous measurement of the force and response signals so that the effect of external forces on the measured response signals could be removed. In addition, when a degree-of-freedom (DOF) response in a position is not exposed to a direct action of any external forces, the response can be selected for the use of the RD technique to obtain force-free RD signatures (Ku *et al*. 2007b). However, when the external force of a real structure is difficult, if not impossible, to well define and accurately measure, special attention should be given to modal parameter identification methods, which may not have to rely on knowing the external force.

A random decrement based method, adopting the assumption of Gaussian white noise and the concept of the traditional frequency response function, has been proposed to deal with singular points in acceleration-based RD signatures (Ku *et al*. 2007a). Nonetheless, a periodic excitation is often present in many practical cases in addition to white noise excitation. When unknown external forces are colored to some extent, the accuracy of the modal parameters identified by a frequency domain identification method is inevitably influenced as well. For this reason, the mode indicator function (MIF) (Breitbach 1973) and the complex mode indication function (CMIF) (Shih *et al*. 1988a, b) were applied to help determine the appropriate number of vibration modes in the RD signatures of a dynamic system for the use of a rational fraction polynomial model (Ku and Tamura 2009).

This paper is aimed at complementing previous studies on solutions to the identification problem in force-embedded acceleration data via a three-stage procedure for modal parameter identification, and demonstrates its application to acceleration response data of a large-span roof structure. Unlike previous studies, the MIF and the CMIF in the procedure are adapted to identify harmonic excitations in the output-only FRF analysis of the correlation-related functions, and the

CMIF is further served as a basis for identifying the modal parameters of a structure. The correlation-related functions can be considered as impulse response functions for the purpose of modal parameter identification (Ibrahim 1977, James *et al*. 1995, Asmussen 1997, Rodrigues *et al*. 2004, Gul and Catbas 2008). The applicability of the identification procedure to correlation functions of force-embedded acceleration data is initially investigated by numerical simulation of a five-floor shear building and a two-dimensional (2D) frame subjected to white noise and harmonic excitations.

The following section describes the singular problem in acceleration-based correlation functions using a state space formulation. The identification procedure for the output-only frequency response functions of the correlation functions is outlined in Section 3. Section 4 introduces the procedure for identifying the modal parameters from the simulated acceleration responses of the five-floor shear building and the 2D frame. Section 5 presents the identified results of the modal parameters of the large-span roof structure that may be excited by harmonic vibrations due to construction work, in addition to various ambient vibrations. Finally, Section 6 presents some conclusions.

2. Singular problem in acceleration-based correlation functions

Demonstration of the singular points in acceleration-based correlation functions starts with the governing equations of motion for a linear and time-invariant n DOF dynamic system that can be expressed in a matrix form as follows

$$\boldsymbol{M}\ddot{\boldsymbol{X}}(t)+\boldsymbol{C}\dot{\boldsymbol{X}}(t)+\boldsymbol{K}\boldsymbol{X}(t)=\boldsymbol{F}(t) \qquad t\geq 0 \tag{1}$$

in which $\boldsymbol{M}$, $\boldsymbol{C}$, and $\boldsymbol{K}$ denote $n\times n$ matrices of mass, damping, and stiffness, respectively, in the dynamic system and $\boldsymbol{F}(t)$ represents an $n\times 1$ vector of external forces. A state space formulation for Eq. (1) is (Hart and Wang 2000)

$$\dot{\boldsymbol{z}}(t)=\boldsymbol{A}\boldsymbol{z}(t)+\boldsymbol{f}(t) \tag{2}$$

where $\boldsymbol{z}(t)=\begin{bmatrix}\boldsymbol{X}(t)\\ \dot{\boldsymbol{X}}(t)\end{bmatrix}_{2n\times 1}$, $\boldsymbol{A}=\begin{bmatrix}\boldsymbol{0}_{n\times n} & \mathbf{I}_{n\times n}\\ -\boldsymbol{M}^{-1}\boldsymbol{K} & -\boldsymbol{M}^{-1}\boldsymbol{C}\end{bmatrix}_{2n\times 2n}$, $\boldsymbol{f}(t)=\begin{bmatrix}\boldsymbol{0}\\ \boldsymbol{M}^{-1}\boldsymbol{F}(t)\end{bmatrix}_{2n\times 1}$

Using the normal mode approach to represent the responses as a superposition of the contributions from each normal mode, the state vector $z(t)$ can be written as

$$\boldsymbol{z}(\mathrm{t})=\boldsymbol{\Psi}\boldsymbol{Q}(\mathrm{t}) \tag{3}$$

in which the modal matrix $\boldsymbol{\Psi} = \begin{bmatrix} \boldsymbol{\phi} & \boldsymbol{\phi}^* \\ \boldsymbol{\phi\lambda} & \boldsymbol{\phi}^*\boldsymbol{\lambda}^* \end{bmatrix}_{2n\times 2n}$ is the eigenvectors of the matrix $\boldsymbol{A}$ and $\boldsymbol{Q}(t) = \begin{bmatrix} \boldsymbol{q}_1(t) & \boldsymbol{q}_2(t) & \dots & \boldsymbol{q}_{2n}(t) \end{bmatrix}^T_{2n\times 1}$ is a new $2n\times 1$ vector of modal coordinates, and the superscripts T and * denote the transposition and the complex conjugate operator, respectively. Substitution of Eq. (3) into Eq. (2) and then pre-multiplication by the inverse of the modal matrix $\boldsymbol{\Psi}^{-1}$ give

$$\boldsymbol{\Psi}^{-1}\boldsymbol{\Psi}\dot{\boldsymbol{Q}}(t) = \boldsymbol{\Psi}^{-1}\boldsymbol{A}\boldsymbol{\Psi}\boldsymbol{Q}(t) + \boldsymbol{\Psi}^{-1}\boldsymbol{f}(t) \tag{4}$$

The modal matrix $\boldsymbol{\Psi}$ has been normalized so as to satisfy the orthogonal condition $\boldsymbol{\Psi}^{-1}\boldsymbol{\Psi} = \boldsymbol{I}$, where $\boldsymbol{I}$ is a $2n\times 2n$ identity matrix. Since each column of $\boldsymbol{\Psi}$ is an eigenvector of $\boldsymbol{A}$, it follows that the other orthogonal condition is

$$\boldsymbol{\Psi}^{-1}\boldsymbol{A}\boldsymbol{\Psi} = \boldsymbol{\Lambda} = diag\begin{bmatrix} \lambda_1 & \lambda_2 & \dots & \lambda_{2n} \end{bmatrix} = \begin{bmatrix} \boldsymbol{\lambda} & 0 \\ 0 & \boldsymbol{\lambda}^* \end{bmatrix}_{2n\times 2n} \tag{5}$$

The matrix $\boldsymbol{\Lambda}$ consists of the eigen-values of $\boldsymbol{A}$ for the n under-damped modes. As a result, Eq. (4) becomes

$$\dot{\boldsymbol{Q}}(t) = \boldsymbol{\Lambda}\boldsymbol{Q}(t) + \boldsymbol{\Psi}^{-1}\boldsymbol{f}(t) \tag{6}$$

A solution of Eq. (6) is given by the convolution integral and the initial conditions

$$\boldsymbol{Q}(t) = \int_{-\infty}^{t} \boldsymbol{e}^{\boldsymbol{\Lambda}(t-\tau)}\boldsymbol{\Psi}^{-1}\boldsymbol{f}(\tau)d\tau + \boldsymbol{e}^{\boldsymbol{\Lambda}t}\boldsymbol{Q}_0 \tag{7}$$

in which $\boldsymbol{Q}_0$ is the modal coordinates related to the initial conditions. Taking advantage of Eq. (3), the forced response of the dynamic system with zero initial conditions is

$$\boldsymbol{z}(t) = \int_{-\infty}^{t} \boldsymbol{s}(t-\tau)\boldsymbol{f}(\tau)d\tau = \int_{0}^{\infty} \boldsymbol{s}(\tau)\boldsymbol{f}(t-\tau)d\tau \tag{8}$$

The zero initial conditions make the final term eliminated from Eq. (7). The state transition matrix $\boldsymbol{s}(t)$ relating $\boldsymbol{z}(t)$ to $\boldsymbol{f}(t)$ is defined as

$$\boldsymbol{s}(t) = \boldsymbol{\Psi}e^{\boldsymbol{\Lambda}t}\boldsymbol{\Psi}^{-1} \tag{9}$$

The first derivative of $\boldsymbol{z}(t)$ with respect to t is obtained as

$$\dot{\boldsymbol{z}}(t) = \int_{-\infty}^{t} \dot{\boldsymbol{s}}(t-\tau)\boldsymbol{f}(\tau)d\tau + \boldsymbol{s}(0)\boldsymbol{f}(t) \tag{10}$$

where

$$\dot{\boldsymbol{s}}(t) = \boldsymbol{\Psi}\boldsymbol{\Lambda}e^{\boldsymbol{\Lambda}t}\boldsymbol{\Psi}^{-1}, \quad \boldsymbol{s}(0) = \mathbf{I}_{2n\times 2n} \tag{11}$$

From Eqs. (8) and (10), it follows that the correlation function matrices of the state space responses are

$$\boldsymbol{R}_{\boldsymbol{zz}}(\tau) = E\left[\boldsymbol{z}(t)\boldsymbol{z}^T(t+\tau)\right] = \int_0^\infty \int_0^\infty \boldsymbol{s}(t_1)\boldsymbol{R}_{\boldsymbol{ff}}(\tau + t_1 - t_2)\boldsymbol{s}^T(t_2)dt_1 dt_2 \tag{12}$$

$$\begin{aligned}\boldsymbol{R}_{\dot{\boldsymbol{z}}\dot{\boldsymbol{z}}}(\tau) = &\int_0^\infty \int_0^\infty \dot{\boldsymbol{s}}(t_1)\boldsymbol{R}_{\boldsymbol{ff}}(\tau + t_1 - t_2)\dot{\boldsymbol{s}}^T(t_2)dt_1 dt_2 + \int_0^\infty \boldsymbol{R}_{\boldsymbol{ff}}(\tau - t_2)\dot{\boldsymbol{s}}^T(t_2)dt_2 \\ &+ \int_0^\infty \dot{\boldsymbol{s}}(t_1)\boldsymbol{R}_{\boldsymbol{ff}}(\tau + t_1)dt_1 + \boldsymbol{R}_{\boldsymbol{ff}}(\tau)\end{aligned} \tag{13}$$

The correlation function matrix of the external force in the final term of Eq. (13) explains the existence of the singular points in the correlation-related functions of acceleration responses, including the acceleration-based RD signature (Huang and Yeh 1999, Ku 2004). For instance, when the external force is white noise, its correlation function is the Dirac delta function giving one singular point to the correlation-related function of the acceleration response. Using such a correlation-related function in a time domain identification method can lead to biased estimates of the modal parameters (Ku *et al*. 2007a, Ku *et al*. 2007b, Ku and Tamura 2009).

3. Identification procedure for frequency response functions of correlation functions

A three-stage identification procedure is proposed to effectively extract the modal parameters from the correlation-related functions of acceleration response data. The fundamental stages of the identification procedure are illustrated in Fig. 1. The procedure comprises the uses of mode indication functions, the enhanced frequency response function, the iterative rational fraction polynomial method, and mode shape inspection.

In the first stage, the potential modes in the FRF matrix of the correlation-related functions are visually detected from plots of MIF and CMIF. MIF and CMIF were originally developed as mode indication functions for traditional multiple-reference FRF data. This study treats the correlation functions as impulse response functions, so that their frequency response functions can result in MIF and CMIF for modal parameter identification. The correlation function in time between the ith and j^{th} displacement responses can be defined by Eq. (14), when a dynamic system is excited by white noise excitations (Cauberghe 2004).

$$\boldsymbol{R}_{ij}(\tau) = \sum_{r=1}^{n}\left[\boldsymbol{\phi}_{ri}e^{\boldsymbol{\lambda}_r\tau}\boldsymbol{C}_{rj} + \boldsymbol{\phi}_{ri}^{*}e^{\boldsymbol{\lambda}_r^{*}\tau}\boldsymbol{C}_{rj}^{*}\right] \tag{14}$$

Based on the definition of Eq. (14), the correlation matrix between n DOF responses and a

subset of the n DOF responses can be transformed to the following FRF matrix

$$\begin{aligned}\boldsymbol{H}_{\boldsymbol{R}}(j\omega) &= \sum_{r=1}^{n}\left(\frac{\boldsymbol{\phi}_r\boldsymbol{C}_r^T}{j\omega-\boldsymbol{\lambda}_r}+\frac{\boldsymbol{\phi}_r^*\boldsymbol{C}_r^H}{j\omega-\boldsymbol{\lambda}_r^*}\right)\\ &= \boldsymbol{\phi}\left[j\omega\boldsymbol{I}_{n\times n}-\boldsymbol{\lambda}\right]^{-1}\boldsymbol{C}^T+\boldsymbol{\phi}^*\left[j\omega\boldsymbol{I}_{n\times n}-\boldsymbol{\lambda}^*\right]^{-1}\boldsymbol{C}^H\end{aligned} \tag{15}$$

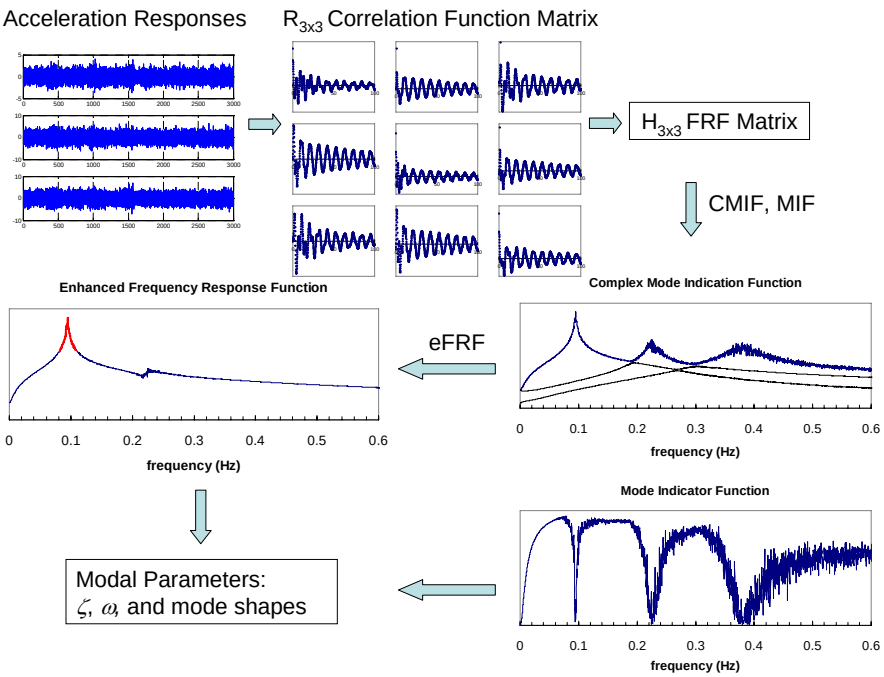

Fig.1 Modal parameter identification procedure for 3DOF acceleration responses

where j is the imaginary unit and ω can be any frequency range of interest. $\boldsymbol{\phi}_r$ and $\boldsymbol{C}_r$ are the eigenvector and the reference vector, respectively, for mode r.

MIF is defined as (Breitbach 1973)

$$\mathbf{MIF}(j\omega)=\frac{\sum_{i=1}^{N_o}\sum_{j=1}^{N_r}\left|\mathrm{Im}\left\{\boldsymbol{H}_{\boldsymbol{R}_{ij}}(j\omega)\right\}\right|\left|\boldsymbol{H}_{\boldsymbol{R}_{ij}}(j\omega)\right|}{\sum_{i=1}^{N_o}\sum_{j=1}^{N_r}\left|\boldsymbol{H}_{\boldsymbol{R}_{ij}}(j\omega)\right|^2} \tag{16}$$

in which N_o is the number of responses and N_r is the number of a subset of the responses. Furthermore, $\mathrm{Im}\{\boldsymbol{H}_{\boldsymbol{R}ij}\}$ and $|\boldsymbol{H}_{\boldsymbol{R}ij}|$ in Eq. (16) are the imaginary part and the magnitude of the FRF, respectively, for the correlation function between $\boldsymbol{x}_i$ and $\boldsymbol{x}_j$. This expression returns a value

between zero and unity, according to the concept of phase resonance. For a specific mode k, Eq. (15) can be approximately reduced to

$$\lim_{\omega \to \omega_k} \boldsymbol{H}_{\boldsymbol{R}}(j\omega) \approx \left(\frac{\boldsymbol{\phi}_k \boldsymbol{C}_k^T}{j\omega - \boldsymbol{\lambda}_k} + \frac{\boldsymbol{\phi}_k^* \boldsymbol{C}_k^H}{j\omega - \boldsymbol{\lambda}_k^*} \right) = 2\,\mathrm{Re}\left(\frac{\boldsymbol{\phi}_k \boldsymbol{C}_k^T}{j\omega - \boldsymbol{\lambda}_k} \right) \tag{17}$$

Eq. (17) gives rise to a real value, when the excitation frequency ω approaches the frequency of a mode. As a result of the real value in Eq. (17), this study shows that a value of zero in the MIF of Eq. (16) can indicate a mode.

CMIF is defined by singular values resulting from singular value decomposition of the FRF matrix at each frequency ω, as shown in Eq. (18) (Shih *et al*. 1988b).

$$\underset{N_o \times N_r}{\boldsymbol{H}_{\boldsymbol{R}}(j\omega)} = \underset{N_o \times N_r}{\boldsymbol{U}(j\omega)} \underset{N_r \times N_r}{\boldsymbol{\Sigma}(j\omega)} \underset{N_r \times N_r}{\boldsymbol{V}(j\omega)^H} \tag{18}$$

where $\boldsymbol{\Sigma}$ is a diagonal matrix of the real positive singular values in descending order, and $\boldsymbol{U}$ and $\boldsymbol{V}$ are unitary matrices containing singular vectors. A plot of CMIF can be formed by singular values as a function of frequency. The largest singular value curve in CMIF is plotted across a frequency range of interest first, and then the subsequent singular value curves are plotted. The resonant peaks detected in the largest singular value curve indicate the existence of potential modes.

When one peak in CMIF can find a corresponding anti-resonance in MIF at the same frequency, each of them can be interpreted as a vibration mode. However, it should be noted that the effect of external forces in the final term of Eq. (13) is also reflected in the FRF matrix of the acceleration-based correlation functions. When harmonic excitations are given to a dynamic system, their frequency components may be mistakenly identified as its dominant modes. On the other hand, the frequency components of the harmonic excitations, like the un-damped modes of the dynamic system, can be distinguished from the damped modes by observing the resonances and anti-resonances in the CMIF and MIF plots, respectively. These resonances and anti-resonances show sharp "jumps" and "drops" corresponding to the frequencies of the harmonic excitations, which are different from showing the frequency response of a damped mode in the plots. Examples in the following numerical simulation will demonstrate how to identify harmonic excitations in CMIF and MIF.

Following the uses of the mode indication functions in the first stage, the second stage in the identification procedure produces information of resonant frequency and scaled mode shape for each mode using a CMIF-based method. This method locates the damped natural frequencies by local maxima in the CMIF plot and, corresponding to these frequencies, determines the approximate mode shapes by the 1st singular vector in $\boldsymbol{U}$. To select the modes that are physically meaningful, visual inspection of the resulting mode shapes is also given in this study.

The third stage produces information of damping ratios by applying a rational fraction polynomial (RFP) method (Pintelon *et al*. 1994) to an enhanced frequency response function (eFRF) (Shih *et al*. 1988b, Fladung *et al*. 2003). The eFRF for the selected mode k is described as follows

$$\underset{1\times 1}{e\hat{\boldsymbol{H}}_k(j\omega)} = \underset{1\times N_o}{\boldsymbol{U}_k^H}\ \underset{N_o\times N_r}{\boldsymbol{H}_{\boldsymbol{R}}(j\omega)}\ \underset{N_r\times 1}{\boldsymbol{V}_k} \tag{19}$$

The 1st singular vectors, $\boldsymbol{U}_k$ and $\boldsymbol{V}_k$, associated with the 1st singular value of mode k in $\boldsymbol{\Sigma}$ are further used to generate the eFRF. In fact, the singular vectors, $\boldsymbol{U}_k$ and $\boldsymbol{V}_k$, play the role of a spatial filter that attenuates the contribution of all modes except the single mode of interest in the eFRF. Therefore, the eFRF can be further analyzed by a simple single-DOF parameter estimation algorithm.

The RFP method can be used to estimate the pole from the eFRF for each mode. The use of the RFP method is to establish a rational fraction polynomial model that curve-fits the eFRF in the frequency range of a mode. The eFRF can be described by the sum of two functions of frequency ω, i.e.

$$e\hat{\boldsymbol{H}}_k(j\omega) = \boldsymbol{H}_k(j\omega) + \boldsymbol{e}_k(j\omega) \tag{20}$$

The true RFP model $\boldsymbol{H}_k(j\omega)$ is expressed by the ratio of two real polynomial coefficients, $\boldsymbol{a}$ and $\boldsymbol{b}$

$$\boldsymbol{H}_k(j\omega_r) = \sum_{i=0}^{2m-2} \boldsymbol{a}_i (j\omega_r)^i \Big/ \sum_{i=0}^{2m} \boldsymbol{b}_i (j\omega_r)^i \qquad r = 1,\ldots, L \tag{21}$$

where m represents the number of vibration modes, L is frequency values, and $b_{2m} = 1$ (He and Fu 2001).

$\boldsymbol{e}(j\omega)$ is treated as an error function in eFRF and this error function is a nonlinear function in terms of eFRF and the polynomial coefficients. Minimization of the error function is a basis to determine the polynomial coefficients of the RFP model. The Newton-Gauss iterative algorithm is thus provided to minimize the nonlinear least squares error function $\boldsymbol{J} = \boldsymbol{e}(j\omega)^T\boldsymbol{e}(j\omega)$, where $\boldsymbol{e}(j\omega) = [e(j\omega_1), \ldots, e(j\omega_L)]^T$ for L frequency values (Pintelon *et al.* 1994). The sth iterative step in the algorithm is given by

$$\left(\partial\boldsymbol{e}/\partial\boldsymbol{\pi}^{(s)}\right)^T \left(\partial\boldsymbol{e}/\partial\boldsymbol{\pi}^{(s)}\right)\Delta\boldsymbol{\pi}^{(s+1)} = -\left(\partial\boldsymbol{e}/\partial\boldsymbol{\pi}^{(s)}\right)^T \boldsymbol{e}^{(s)} \tag{22}$$

where the real coefficients $\boldsymbol{\pi} = [a_0, a_1,\ldots, a_{2m-1}, b_0, b_1,\ldots, b_{2m}]^T$ are to be determined. Due to the iterative feature, an initial estimate of the coefficients is required in the algorithm by means of a least square method.

This study fixes the number of modes m to be 1 for eFRF, leading to the denominator polynomial order of two. To consider the residual effects of out-of-band modes to the frequency range of eFRF, additional numerator polynomial terms can be used in the RFP model (Richardson and Formenti 1982). Therefore, the numerator polynomial order n_u in the RFP model shown in Eq. (23) is gradually increased to enhance the identification accuracy.

$$\boldsymbol{H}_k(j\omega_r) = \sum_{i=0}^{n_u} \boldsymbol{a}_i (j\omega_r)^i \Big/ \sum_{i=0}^{2} \boldsymbol{b}_i (j\omega_r)^i \tag{23}$$

As long as the coefficients, $\boldsymbol{a}$ and $\boldsymbol{b}$, of the RFP model for eFRF are obtained, the natural frequency and damping ratio of mode k can be evaluated by Eq. (24) using the pole of the denominator polynomial.

$$\boldsymbol{\omega}_{nk} = |\boldsymbol{P}_k| \quad , \quad \boldsymbol{\xi}_k = -\mathrm{Real}(\boldsymbol{P}_k)/|\boldsymbol{P}_k| \tag{24}$$

in which $\boldsymbol{P}_k$ is the pole of mode k.

4. Numerical simulation

The applicability of the proposed identification procedure to extracting the modal parameters from acceleration-based correlation functions was investigated through numerical simulation of a five-floor shear building and a 2D frame. To assess the accuracy of the identified results of the natural frequency and damping ratio, a quality measure is defined by the relative error $\varepsilon = |A_k - \hat{A}_k|/A_k \times 100\%$, in which A and $\hat{A}$ are the analytical and identified results, respectively, of mode k. Correlation between the analytical and identified mode shapes at a particular frequency is quantified by the mode assurance criterion (MAC) (Allemang and Brown 1983).

4.1 Example 1: Five-floor shear building

The five-floor shear building shown in Fig. 2 can be depicted by a five-degree-of-freedom linear dynamic model with the following properties: Young's modulus E = 200 GPa, moment of inertia I_z = 36,000 cm^4, floor height L = 3 m, and lumped mass $m = 2\times10^7$ kg. As a result, the mass and stiffness matrices for the shear building are

$$[M] = 2\times10^7 diag[1 \quad 1 \quad 1 \quad 1 \quad 1]\text{kg}, \quad [K] = 10^7 \begin{bmatrix} 12.8 & -6.4 & 0 & 0 & 0 \\ -6.4 & 12.8 & -6.4 & 0 & 0 \\ 0 & -6.4 & 12.8 & -6.4 & 0 \\ 0 & 0 & -6.4 & 12.8 & -6.4 \\ 0 & 0 & 0 & -6.4 & 6.4 \end{bmatrix} \text{N/m}$$

Slight proportional damping with the relation $[C] = 0.0015[M] + 0.0025[K]$ is added to the shear building. The shear building with proportional damping has modes in ascending order at 0.08 Hz, 0.24 Hz, 0.37 Hz, 0.48 Hz, and 0.55 Hz with 0.21%, 0.24%, 0.32%, 0.40%, and 0.45% critical damping.

Two cases of external forces were simulated using Gaussian white noise and a sinusoidal function. Case 1 applies five uncorrelated Gaussian white noise excitations to the floors and a sinusoidal force with a frequency of 0.15 Hz to the middle floor. Case 2 uses one Gaussian white

noise excitation plus the same sinusoidal force on the ground of the shear building so that the forces exciting the floors are fully correlated.

The acceleration responses of the shear building were analyzed using the Newmark-numerical integral method with a linear acceleration algorithm at an interval of 0.1 s in the numerical simulation (Cheng 2000). The total time for each segment of the acceleration responses is 3600 s. 26 individual segments of the responses were generated in each case. A subset of the responses containing all five DOF responses was formed and each of the responses in turn functioned as a reference with respect to the responses for the computation of a correlation matrix. In other words, all DOFs of the responses were used to calculate the correlation matrix having a size of 36,000×5×5×26. The correlation matrix was then transformed into the frequency domain to yield 26 FRF matrices. These 26 FRF matrices were averaged to obtain an FRF matrix with a size of 36,000×5×5.

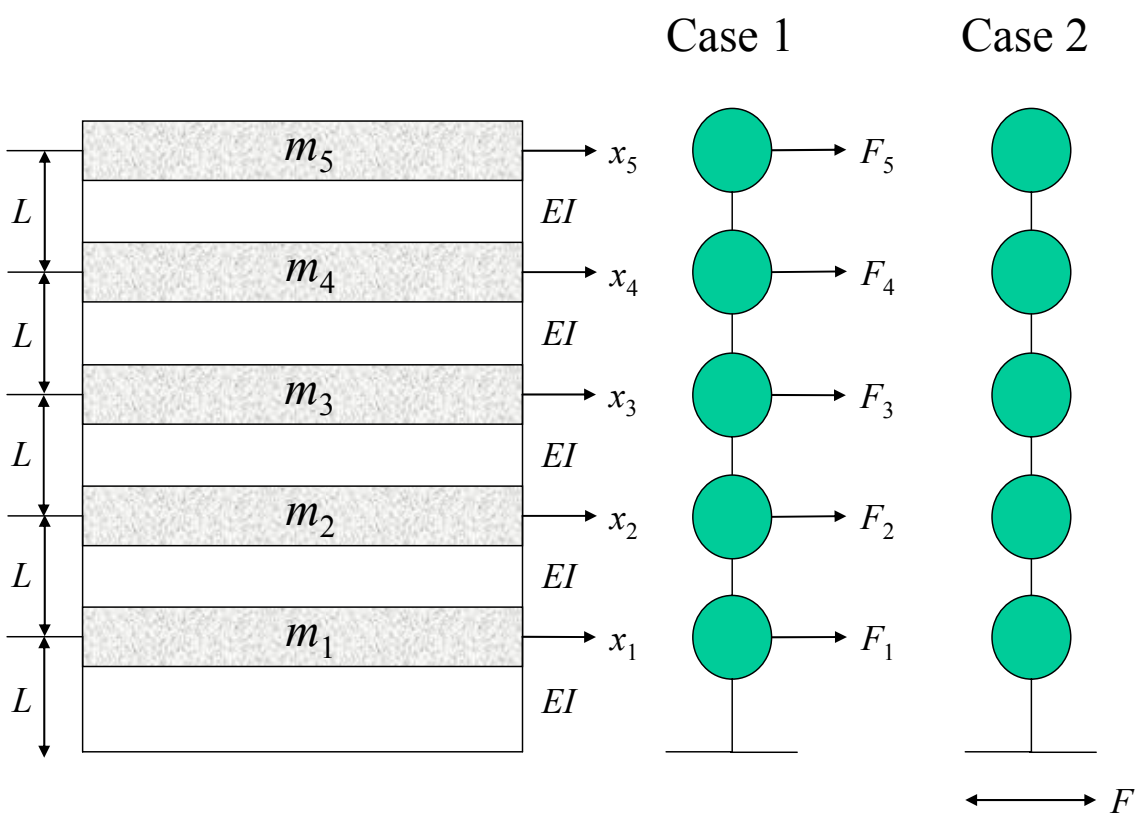

Fig. 2 Five-floor shear building

With the 25 (i.e., 5×5) frequency response functions in the FRF matrix, CMIF and MIF were evaluated. Plots of CMIF and MIF in a frequency range between 0 Hz and 0.6 Hz are shown in Fig. 3, from which the potential modes can be determined. For both cases, a frequency resonance at

0.15 Hz appears in these plots, which reflects the influence of the sinusoidal force in the FRF matrix. Close observation of the resonance and corresponding phase at 0.15 Hz in the plots reveals a clear-cut change, because the Fourier transform of the correlation function of a sinusoidal force is a constant. This change helps identify the sinusoidal force in the acceleration responses. Moreover, inspection of the mode shape relating to the frequency of 0.15 Hz with all analytical mode shapes shows that the MAC values are below 0.05 and, in consequence, this frequency resonance can be ignored. Once the external force is identified from the MIF and CMIF, the 5 modes of the shear building can be located with confidence for each case.

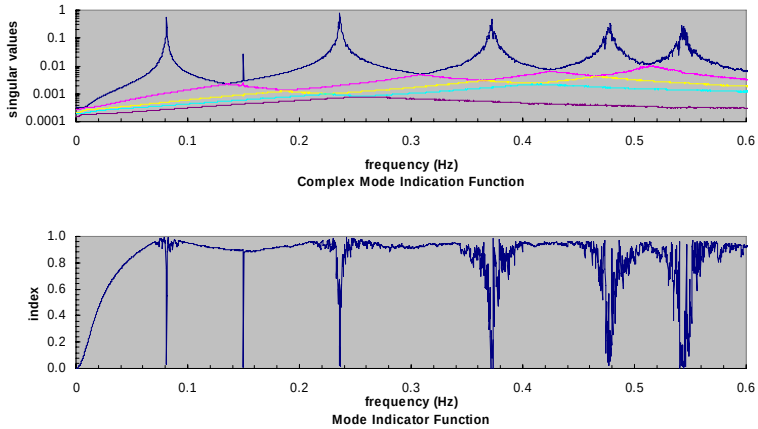

(a) Case 1

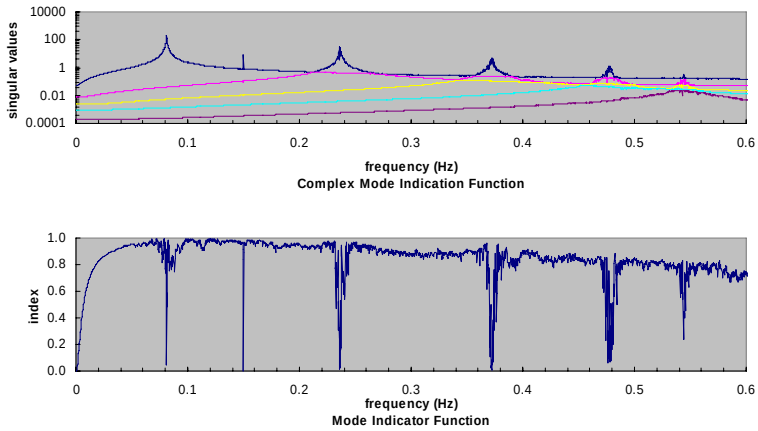

(b) Case 2

Fig. 3 Complex mode indication function and mode indicator function of two cases for a five-floor shear building

Table 1 compares the identified modal parameters of the 5 modes in the shear building with the analytical modal parameters. Results show that the relative errors of the natural frequencies are slight in the two cases. In addition, the MAC values are all larger than 0.99, indicating that the corresponding mode shapes of the identified and analytical results are well correlated. According to the low relative errors and the high MAC values in Table 1, the natural frequencies and corresponding mode shapes can be effectively and reliably identified from the force-embedded acceleration responses by using the CMIF-based method.

Table 1 Identified results in Example 1: a five-floor shear building

Cases	Modes	Natural frequency	Relative error	Damping ratio	Relative error	MAC
Case 1	1	0.08 Hz	0.1%	0.24%	14.9%	1.00
	2	0.24 Hz	0.2%	0.20%	16.1%	1.00
	3	0.37 Hz	0.2%	0.38%	16.1%	1.00
	4	0.48 Hz	0.1%	0.38%	4.6%	1.00
	5	0.54 Hz	0.7%	0.44%	2.1%	1.00
Case 2	1	0.08 Hz	0.1%	0.23%	9.5%	1.00
	2	0.24 Hz	0.3%	0.25%	7.3%	1.00
	3	0.37 Hz	0.2%	0.31%	4.4%	1.00
	4	0.48 Hz	0.2%	0.41%	2.1%	1.00
	5	0.54 Hz	0.5%	0.39%	12.7%	0.99

The estimated damping ratios of the cases are also given in Table 1, after applying the iterative RFP method to the eFRF with the numerator polynomial order of 3 in the RFP model and an isolated window of 81 spectral lines around the natural frequency. The numerator polynomial order of 3 is determined with the aid of stabilization diagrams. Fig. 4 shows examples of stabilization diagrams for case 1, when the numerator order in the RFP model is increased from one to six for every single mode. The trend of the frequency and damping can be observed in Fig. 4, in which the vertical dotted lines represent the analytical natural frequencies and damping ratios of the modes.

The results in Table 1 show that the damping ratios are less accurate than the corresponding

natural frequencies. The range of relative errors in the damping results of the modes varies between 2.1% and 16.1% in the two cases. As a matter of fact, the identification accuracy of the modal parameters is affected not only by the harmonic excitation, but also by the white noise excitation in the acceleration responses. The effect of the white noise excitations over the frequency band, similar to adding white noises in response signals, can lead to numerical error in the modal parameters, especially for the damping estimates, during the computation.

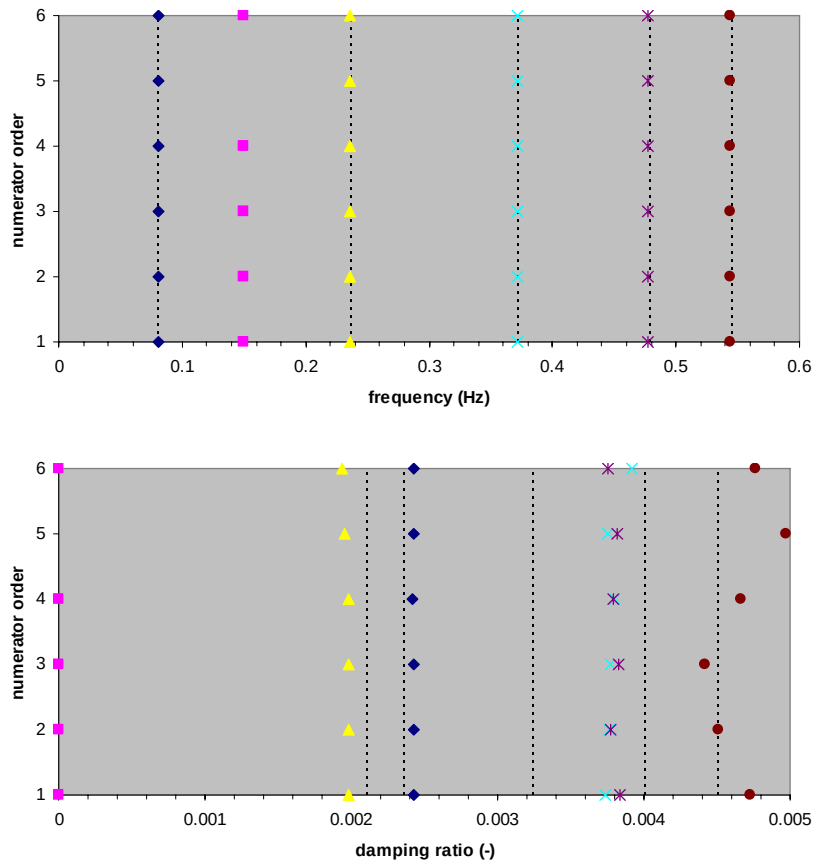

Fig. 4 Stability diagrams of frequency and damping results for case 1; ♦ 1st mode, ▲ 2nd mode, x 3rd mode, * 4th mode, ● 5th mode

4.2 Example 2: Two-dimensional frame

The second example considered is the two-dimensional frame shown in Fig. 5, which is modeled by six beam elements with 18 DOFs. The coordinates of 1, 2, 3, 4, 5, and 6 are fixed ends. The following properties are adopted: Young's modulus E = 200 GPa, cross section area = 0.001 m^2, moment of inertia I_z = 36000 cm^4, length of beam L = 3 m, and mass per length m = 4.5×10^7 kg/m. The evaluation of proportional damping uses the same relation as the previous example.

The analytical results of the modal parameters in the frame are listed in Table 2. To generate the 26 segments of the acceleration responses, the white noise excitations were loaded to the coordinates of 7, 10, 13, 14, 16, and 17, while the sinusoidal force was loaded to the coordinate of 7. A subset of the responses was selected at the coordinates of 13, 14, 15, and 16 to obtain a correlation matrix with the size of 36,000×12×4×26 and an FRF matrix with the size of 36,000×12×4.

Table 2 Identified results in Example 2: a two-dimensional frame

Modes	Natural frequencies			Damping ratios			MAC
	Identified results	Analytical results	Relative error	Identified results	Analytical results	Relative error	
1	0.03 Hz	0.03 Hz	0.22%	0.58%	0.49%	19.81%	1.00
2	0.07 Hz	0.07 Hz	0.08%	0.23%	0.23%	0.45%	1.00
3	0.09 Hz	0.09 Hz	0.03%	0.18%	0.20%	13.66%	1.00
4	0.13 Hz	0.13 Hz	0.11%	0.22%	0.19%	15.35%	1.00
5	0.16 Hz	0.16 Hz	0.14%	0.15%	0.20%	27.62%	1.00
6	0.19 Hz	0.19 Hz	0.04%	0.20%	0.21%	6.20%	1.00
7	0.25 Hz	0.25 Hz	0.08%	0.23%	0.24%	5.43%	1.00
8	0.26 Hz	0.26 Hz	0.08%	0.23%	0.25%	9.29%	1.00
9	0.41 Hz	0.41 Hz	0.48%	0.36%	0.36%	0.47%	1.00
10	0.51 Hz	0.51 Hz	0.29%	0.43%	0.42%	0.70%	1.00
11	0.57 Hz	0.57 Hz	0.57%	0.45%	0.47%	2.94%	1.00
12	0.98 Hz	1.00 Hz	1.72%	0.78%	0.80%	2.32%	1.00

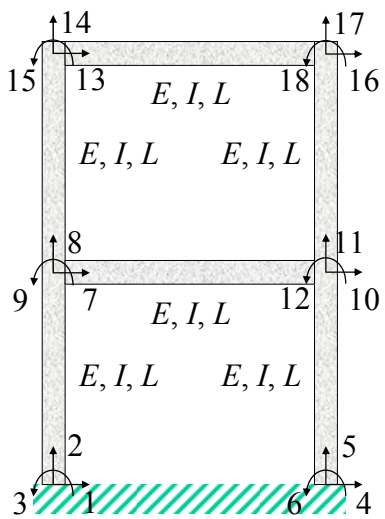

Fig. 5 A two-dimensional frame with 18 degrees of freedom

The CMIF and MIF of the FRF matrix are illustrated in Fig. 6, in which 12 modes between 0 Hz and 1.2 Hz can be found. Table 2 compares the identified modal parameters of the 12 modes

with the analytical modal parameters. The comparison reveals excellent agreement. Still, the estimated damping ratios lack accuracy when the numerator polynomial order in the RFP model is set as 1 and the isolated window for each mode contains 81 spectral lines. It is shown that the relative error of the estimated damping ratio in each mode is higher than that of the corresponding natural frequency. In particular, the relative error of the 5th damping ratio reaches 27%, while the relative error of the 5th natural frequency at 0.16 Hz is only 0.14%. In addition to the effect of the white noise excitation as previously mentioned, the existence of the sinusoidal force at the frequency of 0.15 Hz, in close proximity to the frequency of the 5th damping ratio, is a major cause of the high relative error. Therefore, wide separation between the harmonic excitations and the vibration modes is required for the estimate of damping ratios when using the proposed identification procedure.

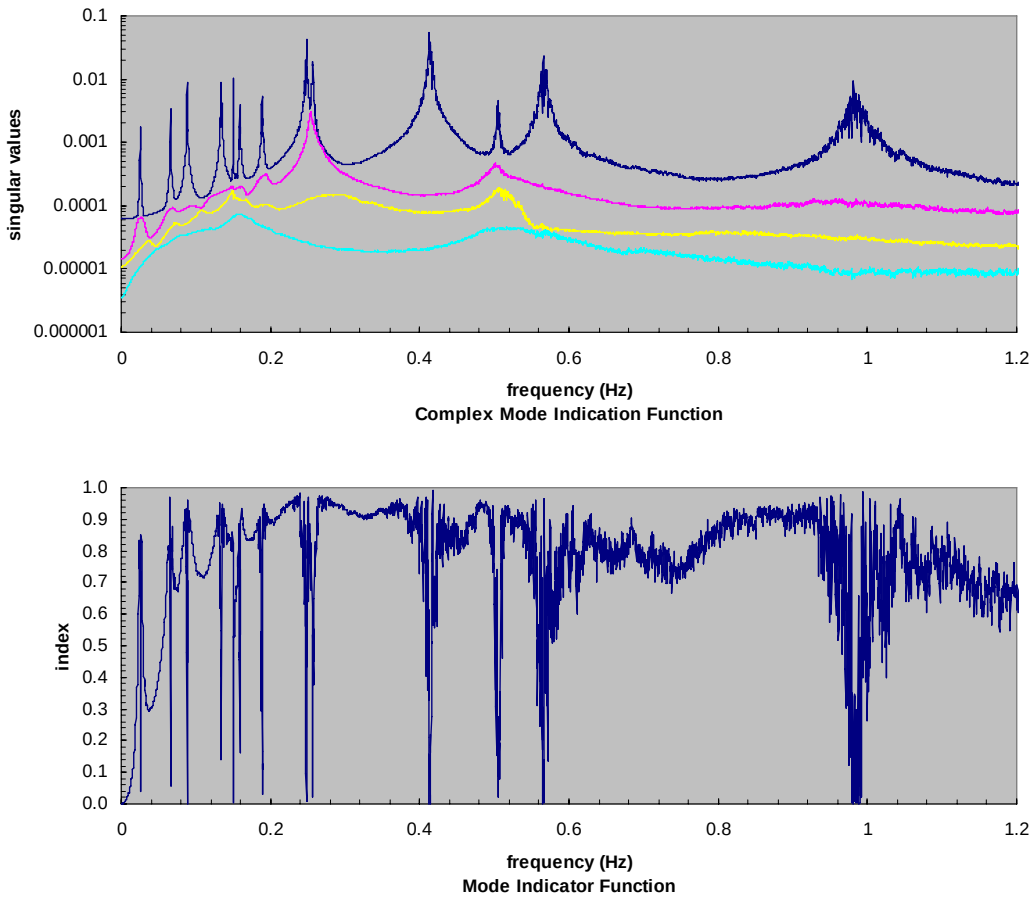

Fig. 6 Complex mode indication function and mode indicator function of a two-dimensional frame

5. Application of identification procedure to large-span roof structure

5.1 Description of a roof structure

A large-span roof structure was built over a six-story grandstand at the Tokyo horse race stadium, Japan, in 2007 as part of its renovation. This structure was required to cover large areas of the grandstand to create a secure and comfortable environment. Fig. 7 shows a photograph of this structure after the first stage of a three-stage construction, which was selected in this study for ambient vibration tests. The structure is 108 m long, 49 m wide and 42.8 m high.

11 pairs of longitudinal girders frame the roof structure in a cantilever form. Each pair is connected with transverse beams. The clear span between two pairs of girders is 10.8 m, and they are transversally connected with cross- and X-shaped struts. A folded steel decking lies on top of the roof structure. Louvers and fins stick out of the decking, and assist in controlling the aero-stability of the roof structure. In addition, a cable-stayed system transfers the roof loads to masts through tension cables that cope with the instability when taking on compression loads for wind uplift.

Fig. 7 A large-span roof structure

5.2 Ambient vibration testing

Ambient vibration testing has been an efficient experimental vibration method for determining the dynamic properties of full-scale structures in recent decades. Vibration responses can be collected via ambient vibration tests while a structure is being subjected to the forces of nature such as winds, micro-tremors, or other natural excitations. A grid of 51 test locations on the rooftop of the structure along the cantilever girders, as shown in Fig. 8, was selected for the ambient vibration tests. The vertical acceleration responses of the roof structure under consideration were measured using 15 uni-axial servo-type accelerometers. Of these accelerometers, three were fixed to respective reference locations during the tests and the rest were assigned as roving sensors in four individual measurement setups. They had a nominal sensitivity of 1000 mV/g and an effective frequency band from 0 Hz to 100 Hz. Each was mounted on a

base plate to ensure proper alignment.

Acceleration response signals in each measurement setup were simultaneously recorded by four portable PC-based data acquisition systems. The sampling frequency in the systems was set to 100 Hz per channel, at least 10 times the maximum frequency of interest. To eliminate all high-frequency noises, the cut-off frequency of an analogue anti-aliasing filter in each data acquisition system was selected at 10 Hz per channel. Each ambient vibration test collected 30-minute response data, corresponding to 180,000 sampling points at each test location. The measured acceleration response data from the four measurement setups, 3 with 15 channels and 1 with 12 channels, were used in the following ambient vibration analysis.

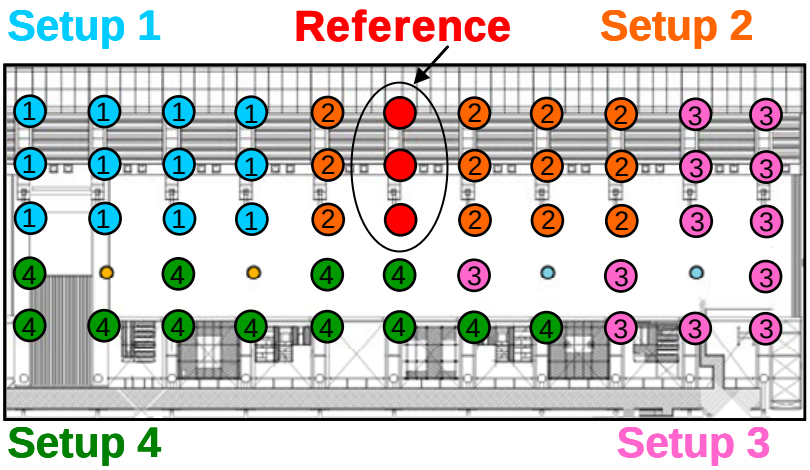

Fig. 8 Measurement setups on the rooftop

5.3 Ambient vibration analysis

The identification procedure was applied to the correlation matrix evaluated between the channels of the measured response data and a subset of the channels in each measurement setup. To avoid missing vibration modes in the identification procedure due to the proximity of the reference locations to nodes of these modes, the subset of the channels specified the response data measured at 6 of the test locations, including the 3 stationary reference locations. The measured data were further divided into 20 time segments with a 50 percent overlap between contiguous segments and a length of 16,384 sampling points in each segment for the computation of a correlation matrix. For example, the correlation matrix with the size of 16,384×15×6×20 was formed from the three data sets using the 15 data channels.

An averaged FRF matrix having a size of 16,384×15×6 and a frequency resolution of 0.006 Hz was obtained, after transforming the correlation matrix into the frequency domain. The averaged FRF matrix was further used to evaluate the CMIF and MIF for each data set. This means that the identification procedure processed the four data sets one at a time, and then the related results of the four data sets were combined. The averaged and normalized CMIF and the averaged MIF in the frequency range from 1 to 5 Hz are illustrated in Fig. 9. Approximately 14 vertical modes of

vibration were detected in the plots of the CMIF and MIF, in which a red square marks each of the detected modes.

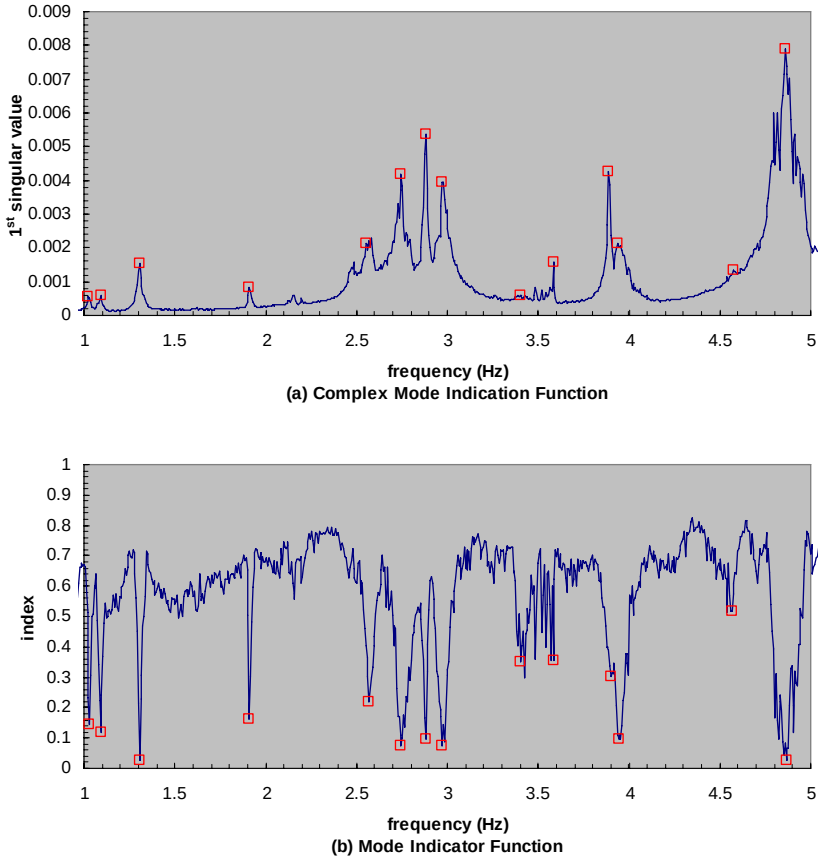

Fig. 9 Averaged results from four data setups for (a) complex mode indication function and (b) mode indicator function; □ selected frequency

Table 3 lists the mean value and the difference between the maximum and minimum of the identified results for each of the 14 modes. The resonant frequencies and corresponding mode shapes from the FRF matrix in each data set were identified by the CMIF-based method. The identified frequencies can be considered to have a high degree of consistency because of the low variances in the results of the four data sets. For the 14 frequencies, the complete modal deflection shapes were compiled from the mode shape components of the four individual data sets. The mode shape components at untested locations were interpolated by those from the tested locations using the Kriging method. Fig. 10 shows the real part of the modal deflection shapes for the modes.

After determining the modes, the iterative RFP method was applied to the eFRF for the damping estimate of each mode. The numerator polynomial order in the RFP model was increased from one to six for every single mode containing spectral lines. The range of the spectral lines was

evaluated using the MAC value above 0.85 between the 1st singular vector at the resonant frequency and the singular vectors at the frequencies around the mode. The estimated damping ratios from the four data sets are shown in Table 3, where the numerator polynomial order n_μ used in Eq. (23) is 5. It is found that the range of the estimated damping ratios for each mode is quite wide, which indicates a high degree of uncertainty in the damping estimates. One reason for this result is the effect of amplitude dependence due to damping values changing with vibration amplitude (Jeary 1986, Tamura and Suganuma 1996, Pirnia *et al*. 2007). In addition, there are other nonlinear characteristics that contribute to uncertainties in damping estimates, such as aero-elastic interactions and complex damping mechanisms in the structure.

Table 3 Identified natural frequencies and damping ratios from acceleration response data of a roof structure

Modes	Natural frequencies		Damping ratios	
	Mean	Difference	Mean	Difference
1	1.03 Hz	0.01 Hz	0.72%	0.48%
2	1.09 Hz	0.00 Hz	0.90%	0.42%
3	1.30 Hz	0.01 Hz	0.64%	0.30%
4	1.91 Hz	0.01 Hz	0.30%	0.23%
5	2.55 Hz	0.01 Hz	0.70%	0.88%
6	2.75 Hz	0.02 Hz	0.85%	1.07%
7	2.88 Hz	0.01 Hz	0.25%	0.18%
8	2.98 Hz	0.01 Hz	0.82%	0.20%
9	3.39 Hz	0.02 Hz	0.07%	0.13%
10	3.58 Hz	0.02 Hz	0.12%	0.25%
11	3.89 Hz	0.01 Hz	0.18%	0.19%
12	3.94 Hz	0.01 Hz	0.63%	0.24%
13	4.58 Hz	0.01 Hz	0.08%	0.11%
14	4.86 Hz	0.02 Hz	1.14%	0.44%

Note: Difference = maximum – minimum

6. Conclusions

This paper has addressed a parameter identification problem of a dynamic system resulting from the use of forced acceleration responses, when external forces are not available. The problem is attributed to an external force imparted to its impulse acceleration response function, as shown in Eq. (10). The problem can have an impact on the identification accuracy of the modal parameters when using the forced acceleration responses in a modal parameter identification technique. This may restrict the practical value and applicability of the acceleration responses to modal parameter identification, while acceleration measurement is crucially important to wind-excited structures and in other engineering fields.

A three-stage identification procedure has been provided as a solution to the identification problem in the presence of harmonic and white noise excitations. The identification procedure

applies mode indication functions, the enhanced frequency response function, the iterative rational fraction polynomial method, and mode shape inspection to the output-only FRF matrix of the acceleration-based correlation functions. In this study, CMIF and MIF have been derived from the correlation functions of the force-embedded acceleration responses to detect not only the vibration modes but also the harmonic excitations.

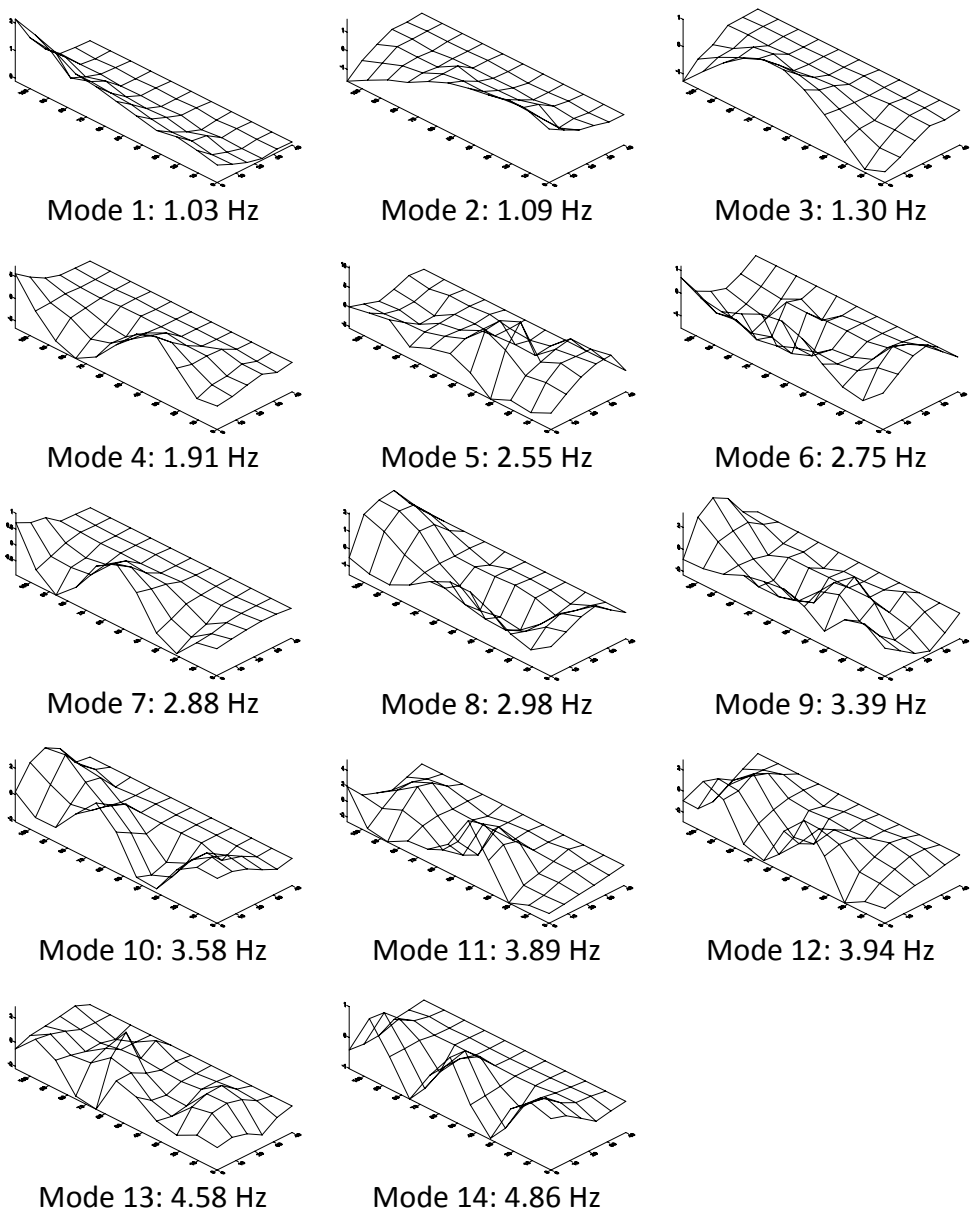

Fig. 10 14 modal deflection shapes of a roof structure

The performance of the identification procedure has been investigated via the numerical simulation of a five-floor shear building and a 2D frame, subjected to white noise and harmonic excitations. Simulation results have provided strong evidence of the harmonic excitation existing in the forced acceleration responses by observing the clear-up jump and drop in the plots of CMIF and MIF. Once identifying the harmonic excitation in the plots, the modal parameters of a structure can be effectively extracted from the force-embedded acceleration responses. Similarly, the identification procedure can also expand its use to a 3D linear dynamic system under white noise and harmonic excitations. It is notable that the use of the procedure, like other developed identification procedures, has its own limitation. It requires wide separation between vibration modes and harmonic excitations. When the frequencies of the vibration modes and the harmonic excitations are in close proximity to each other, the identification accuracy of the modal parameters resulting from the force-embedded acceleration responses are affected.

The applicability of the procedure to measured acceleration response data of a large-span roof structure excited by ambient vibrations has also been evaluated. 14 vibration modes have been located in the mode indication functions, CMIF and MIF, between 1 Hz and 5 Hz. The results of the natural frequency and modal deflection shape for the 14 modes have been satisfactorily identified using the proposed procedure to measured response data. Though the damping results provided by this study are very variable, the mean values of the results over the four data sets are likely to be representative of the effective damping ratios in the roof structure under varying environmental and operational conditions.

Acknowledgements

The writers would like to express their gratitude to Mr. Takayuki Komi for his assistance in conducting ambient vibration tests and to Dr. Lu Guo and Mr. Zhibin Ding for their invaluable comments on this work. The sponsorship of the Ministry of Education, Culture, Sports, Science and Technology, Japan, through the Global Center of Excellence Program, 2008-2013, is gratefully acknowledged.

References

Allemang, R.J. and Brown, D.L. (1983), "A correlation coefficient for modal vector analysis", *Proceedings of the 1st International Modal Analysis Conference*, Union College, Orlando, Florida.

Asmussen, J.C. (1997), *Modal Analysis Based on the Random Decrement Technique*, Ph.D. Thesis, Aalborg University, Aalborg, Denmark.

Bedewi, N.E. (1986), *The Mathematical Foundation of the Auto and Cross-Random Decrement Techniques and the Development of a System Identification Technique for the Detection of Structural Deterioration*, Ph.D. Thesis, University of Maryland, College Park, Maryland, USA.

Breitbach, E. (1973), "A semi-automatic modal survey test technique for complex aircraft and spacecraft structures", *Proceedings of the 3rd ESRO Testing Symposium*, Frascati, Italy.

Cauberghe, B. (2004), *Applied Frequency-Domain System Identification in the Field of Experimental and Operational Modal Analysis*, Ph.D. Thesis, Vrije Universiteit Brussel, Brussels, Belgium.

Cheng, F.Y. (2000), *Matrix Analysis of Structural Dynamics Applications and Earthquake Engineering*, Marcel Dekker, New York, USA.

Cole, H.A. (1971), *Method and apparatus for measuring the damping characteristic of a structure*, United

State Patent, No. 3,620,069.

Fladung, W.A., Phillips, A.W. and Allemang, R.J. (2003), "Application of a generalized residual model to frequency domain modal parameter estimation", *J. Sound Vib.*, **262**(3), 677-705.

Gul, M. and Catbas, F.N. (2008), "Ambient vibration data analysis for structural identification and global condition assessment", *J. Eng. Mech.- ASCE*, **134**(8), 650-662.

Hart, G.C. and Wong, K. (2000), *Structural Dynamics for Structural Engineers*, John Wiley & Sons, New York, USA.

He, J.M. and Fu, Z.F. (2001), *Chapter 8. Modal analysis methods-frequency domain*, *Modal Analysis*, Butterworth-Heinemann, Oxfort, UK, 174-176.

Huang, C.S. and Yeh, C.H. (1999), "Some properties of randomdec signatures", *Mech. Syst. Signal Pr.*, **13**(3), 491-507.

Ibrahim, S.R. (1977), "Random decrement technique for modal identification of structures", *AIAA J.*, **14**(11), 696-700.

James, G.H., Carne, T.G. and Lauffer, J.P. (1995), "The natural excitation technique (NExT) for modal parameter extraction from operating structures", *J. Anal. Exper. Modal Anal.*, **10**(4), 260-277.

Jeary, A.P. (1986), "Damping in tall buildings - a mechanism and a predictor", *Earthq. Eng. Struct. D.*, **14**(5), 733-750.

Ku, C.J. and Tamura, Y. (2009), "Rational fraction polynomial method and random decrement technique for force-excited acceleration responses", *J. Struct. Eng.- ASCE*, **135**(9), 1134-1138.

Ku, C.J., Cermak, J.E., and Chou, L.S. (2007a), "Random decrement based method for modal parameter identification of a dynamic system using acceleration responses", *J. Wind Eng. Ind. Aerod.,* **95**(6), 389-410.

Ku, C.J., Cermak, J.E. and Chou, L.S. (2007b), "Biased modal estimates from random decrement signatures of forced acceleration responses", *J. Struct. Eng.- ASCE*, **133**(8), 1180-1185.

Ku, C.J. (2004), *Random Decrement Based Method for Parameter Identification of Wind-Excited Building Models using Acceleration Responses*, Ph.D. Thesis, Colorado State University, Fort Collins, Colorado, USA.

Pintelon, R., Guillaume, P., Rolain, Y., Schoukens, J. and van Hamme, H. (1994), "Parametric identification of transfer functions in the frequency domain - a survey", *IEEE T. Automat. Contr.*, **39**(11), 2245-2259.

Pirnia, J.D., Kijewski-Correa, T., Abdelrazaq, A., Chung, J. and Kareem, A. (2007), "Full-scale validation of wind-induced response of tall buildings: investigation of amplitude-dependence dynamic properties", *Proceedings of the Structures Congress 2007*: *New Horizons and Better Practices*, *ASCE*, Long Beach, California, USA, May, 38-47.

Richardson, M.H. and Formenti, D.L. (1982), "Parameter estimation from frequency response measurements using rational fraction polynomials", *Proceedings of the 1st International Modal Analysis Conference*, Union College, Orlando, Florida.

Rodrigues, J., Brincker, R. and Andersen, P. (2004), "Improvement of frequency domain output only modal identification from the application of the random decrement technique", *Proceedings of the 22nd International Modal Analysis Conference*, Dearborn, Michigan.

Shih, C.Y., Tsuei, Y.G., Allemang, R.J. and Brown, D.L. (1988a), "A frequency domain global parameter estimation method for multiple reference frequency response measurements", *Mech. Syst. Signal Pr.*, **2**(4), 349-365.

Shih, C.Y., Tsuei, Y.G., Allemang, R.J. and Brown, D.L. (1988b), "Complex mode indication function and its applications to spatial domain parameter estimation", *Mech. Syst. Signal Pr.*, **2**(4), 367-377.

Tamura, Y. and Suganuma, S. (1996), "Evaluation of amplitude-dependence damping and natural frequency of buildings during strong winds", *J. Wind Eng. Ind. Aerod.*, **59**(2-3), 115-130.

Vandiver, J.K., Dunwoody, A.B., Campbell, R.B. and Cook, M.F. (1982), "A mathematical basis for the random decrement vibration signature analysis technique", *J. Mech. Design*, **104**, 307-313.